Development of Spatiotemporal Population Receptive Field Models (pRF) for the Somatosensory Cortex: an fMRI study

Master Thesis Artificial Intelligence

Martijn Thio

1st supervisor UU: dr. Ben Harvey
2nd supervisor UU: dr. Chris Janssen
UMC supervisor: dr. Wouter Schellekens
UMC supervisor: dr. Natalia Petridou
Utrecht University
July 2019

Abstract

Understanding the topographic organization of the somatosensory cortex is essential in broadening our knowledge on tactile processing. The current study extends the population Receptive Field (pRF) approach first used in visual field mapping studies to create detailed topographic maps of the somatosensory cortex. Specifically, we investigated the receptive fields on the skin of neuronal populations in Brodmann areas 3b, 1 and 2 of the primary somatosensory cortex (S1) to produce such maps. We therefore developed a model that predicted neuronal responses to vibrotactile stimulation of the fingertips. The model was fit on data obtained by functional magnetic resonance imaging (fMRI). We report pRF estimates in the location of the cortical hand area of S1 along the postcentral gyrus corresponding to locations on the skin to which a neuronal population responds. A somatotopic organization of the finger digits was found in BA 3b and 1, but not in B2. We also found that pRFs were larger in BA 2 in comparison to BA 3b and 1. Additionally, we investigated whether a frequency dependency on neuronal responses existed in S1 by running three experiments which differed in frequency. No effect of frequency on neural responses could be found. Nevertheless, our results show that using pRF models can result in detailed maps of the somatosensory cortex including underlying characteristics

Contents

Introduction

Touch is an important source of information humans use to perceive and interact with the world around them. By sensing the differences in pressure while handling objects, human beings (and to some extent other primates) are able to manipulate these objects actively and use them as tools. Through scanning over a surface, information about its texture can be perceived, especially by using the fingers. This for instance enables blind people to read braille. Furthermore, items can be easily recognized in less than two seconds by only using tactile information like weight, shape, size, density and texture (Klatzky, Lederman, and Metzger 1985). Those that suffer from a loss of touch sensation are greatly impaired, such that even everyday tasks like buttoning a shirt or drinking from a cup will become too difficult (Rothwell et al. 1982; Robles-De-La-Torre 2006).

Researching how touch is processed in the brain will not only improve our knowledge on how we observe our environment but will also enable us to better assist those that are afflicted by sensory loss in this domain. Moreover, it can help to create new technologies that benefit from the use of tactile information, such as sensory prosthetics (Antfolk et al. 2013), somatosensory virtual reality (Pamungkas and Ward 2016), tactile feedback in robotic surgery (Pacchierotti, Prattichizzo, and Kuchenbecker 2015) and brain computer interfaces (BCI) based on touch (Herweg et al. 2016). In the domain of autonomous robots, knowledge on the subject is also of value. As all sensory modalities are important for humans in certain areas, equipping robots with similar capacities is essential in making them fully autonomous. However, tactile processing in robots has not been given as much attention compared to other sensory modalities (e.g. vision), mainly due to its complexity (Dahiya et al. 2010). Investigating how humans process touch could therefore contribute to the development of fully autonomous robotic systems.

Most studies on tactile processing direct their attention on the surface of the hand, specifically the fingers, to provide a general description of tactile sensation (Johansson and Vallbo 1983; Greenspan and LaMotte 1993; Abraira and Ginty 2013). This is logical as these are the body parts strongly associated with touch and most important when manipulating objects. For that reason, the current study will mainly focus on the hands and fingers.

Physiology of the Somatosensory System

The sense of touch is part of the somatosensory system, which is concerned with processing all sensations either inside the body or on its surface. It serves three major functions: proprioception, the sense of oneself, exteroception, the sense of external stimuli that interact with the body, and interoception, the sense of the internal state of the body and function of the organs (Kandel et al. 2000). The sense of touch can be described as sensations caused by external mechanical forces on the skin and is, thus, a form of exteroception. Other forms are thermal sensation and the sense of pain, or nociception, which are mostly processed separately (Lumpkin and Caterina 2007). Each type of sensory stimulus activates a different kind of sensory neuron, called a receptor (Iggo and Andres 1982). So how are tactile stimuli detected on the skin and subsequently processed?

The receptors that handle tactile information are called mechanoreceptors and are distributed all over the body. By transferring mechanical pressure or distortions to these receptors tactile sensory information is transmitted through afferent neurons to the central nervous system (CNS), which contains the spinal cord and the brain (Abraira and Ginty 2013). There are four main types of cutaneous (i.e. within the skin) mechanoreceptors involved in processing tactile stimuli which are present in the glabrous skin of the hand. They are classified by the mechanical force they respond to: Merkel corpuscles detect light touch and sustained pressure; Ruffini corpuscles respond mostly to skin stretch; Meissner corpuscles detect texture and low frequency vibrational stimulation in the range 5-50 Hz (also called flutter); Pacinian corpuscles detect high frequency vibrational stimulation in the range of 50-500 Hz, with its strongest response at 200 Hz (Johnson 2001; McGlone and Reilly 2010). Other types include hair follicles, free nerve endings and subcutaneous mechanoreceptors, like muscle spindles, but we will only consider the main mechanoreceptors in the present study. More specifically, we focus on the mechanoreceptors involved in processing vibrotactile stimulation, i.e. Meissner and Pacinian corpuscles. The area of the skin for which an individual mechanoreceptor conveys information is known as its receptive field (Johansson and Vallbo 1983). Eventually, the afferent neurons of all mechanoreceptors project this information to an area of the brain along the postcentral gyrus called the primary somatosensory cortex (S1), mostly on the contralateral side (Tamè et al. 2012).

S1 consists of four distinct cytoarchitectonic structures, namely Brodmann areas (BA) 3a, 3b, 1 and 2, which are respectively distributed from anterior to posterior (Geyer, Schleicher, and Zilles 1997). Like mechanoreceptors, neurons in S1 have a certain receptive field reflecting the part of the

skin to which they respond (Clark et al. 1988). Cortical representations of body parts in S1 follow a somatotopic organization first described roughly by Penfield's homunculus (Penfield and Boldrey 1937). It is ordered from the toes at the top of the cerebral hemisphere down to the mouth (see figure 1). The size of each representation in S1 is proportional to the number of mechanoreceptors in the skin of its corresponding body part and how densely they are distributed (Sur, Merzenich, and Kaas 1980). The hands and fingers therefore have one of the largest cortical representations. Although Penfield's somatotopic arrangement allocates each body part to a certain brain area, it is not yet very detailed. Gaining a better understanding of the topographic organization of S1 is essential in understanding the processing of tactile stimuli as a whole. In Penfield and Boldrey's (1937) ground-breaking study, the researchers electrically stimulated parts of S1 directly on the cortex in patients undergoing brain surgery and simply asked them to report on where they perceived the stimulus (Penfield and Boldrey 1937). A more robust approach is measuring neuronal activity in response to tactile stimulation, which results in more detailed maps of somatosensory regions of the brain.

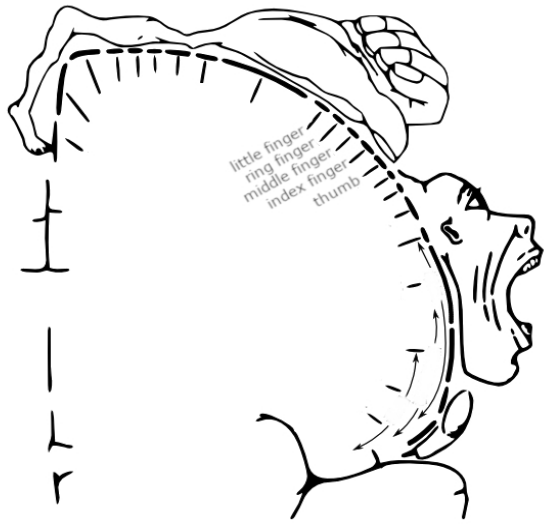

Figure 1: Homunculus. The order of the body parts along the postcentral gyrus. (Penfield and Boldrey 1937)

Kaas and colleagues (1979) conducted more such experiments using macaque monkeys, because the brains of these non-human primates share many similarities with humans. They placed micro-electrodes directly on the monkey's cortex and measured the electrical activity after stimulating different parts of the body. Their results revealed that the four cytoarchitectonic structures all had independent representations of the body parts. Moreover, they found that the fingers were represented from the thumb most inferior to the little finger most superior. Subsequent studies on non-human primates found that the receptive fields of neurons in BA 3b and 1 were mostly confined to a single finger digit, while neurons in BA 2 responded to up to five digits (Iwamura, Tanaka, and Hikosaka 1980). They concluded that representations of fingers in BA 3 and 1 showed a clear somatotopic organization, while the representations in BA 2 overlapped and did not exhibit such a somatotopy.

Thus, when a tactile stimulus contacts the skin it activates neurons in the contralateral S1 which have their receptive fields covering that particular area. Studies using monkeys have produced detailed somatotopic maps and discovered differences in receptive field sizes between the cytoarchitectonic areas of S1. Although the human brain shares many similarities with that of non-human primates, differences do exist which are not yet well understood (Kaas 2004). However, microelectrode studies require major surgery and are, thus, undesirable. Therefore, a non-invasive technique like functional magnetic resonance imaging (fMRI) is preferred.

fMRI and the Human S1

fMRI is an imaging technique that is used to estimate neural activity based on local hemodynamic changes in the brain (Logothetis 2008). Active neurons in the brain require oxygen, which is delivered by blood flowing into the affected area (Iadecola 2004). Oxygenated and deoxygenated blood differ in their magnetic susceptibility, which produces the blood-oxygen-level-dependent (BOLD) signal (Ogawa et al. 1990). The influx of oxygenated blood in the region increases the signal, which is known as the BOLD response. This response occurs 4-8 seconds after the increase in neural activity but is highly predictable and summarized in a hemodynamic response function (HRF, see figure 2). The BOLD signal can be measured using an MRI scanner and often correlates strongly with neural activity (Ekstrom 2010). By taking repeated measurements over time, four dimensional (x, y, z and time) images can be created where where each data point in an image, called a voxel, contains a time series which reflects changes in activity of an underlying group of neurons. These changes in neural activity are depicted in a voxel's fMRI timeseries. During fMRI experiments neural responses to different stimuli are measured using this technique. The resulting data is commonly analyzed using methods estimating the most effective stimulus for each voxel, often

using a general linear model (GLM). These estimations are then used to produce maps depicting activation patterns in a specific region of the brain. A more extensive discussion on the principles of fMRI research and analysis can be found in the supplementary appendix.

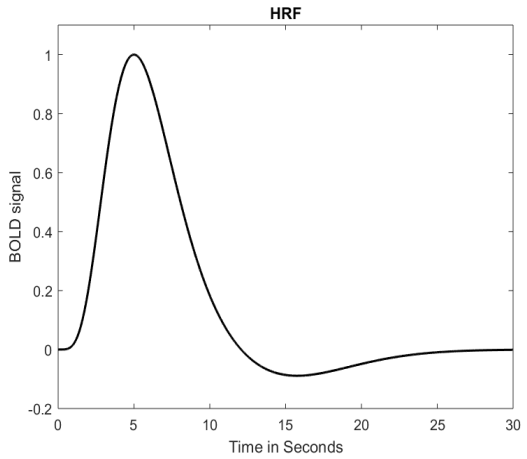

Figure 2: Hemodynamic Response Function. This figure depicts the increase of the BOLD signal after neural activity. The spike occurs around 4-8 s after the increase of activity. After enough oxygen is supplied it returns to baseline.

Several fMRI studies that investigated S1 in the human brain were able to distinguish somatotopic maps of the finger digits by stroking the hands of the subjects while they were in the scanner (Van Westen et al. 2004; Martuzzi et al. 2014). Similar to the non-human primate studies, they found that the digits were organized from the thumb most anterodorsally and inferiorly up to the little finger most posteromedially and superiorly. Moreover, the study by Martuzzi and colleagues (2014) found that selectivity to a single finger was most prominent in BA 3b, while less so in BA 1 and BA 2. This again is indicative of the possibility that cortical representations of the fingers in BA 2 might overlap. Research using vibrotactile stimuli on the fingertips has also been able to produce activity maps in S1, where the organisation of the fingers was similar to that found in the hand stroking studies (Rosa Maria Sanchez-Panchuelo et al. 2010; Besle et al. 2014). A study on a single finger digit was also able to observe activation patterns in areas corresponding to BAs 3a, 3b 1 and 2 following vibrotactile stimulation (Rosa M Sanchez-Panchuelo et al. 2012). Thus, these fMRI studies investigating cortical representations in S1 found similar somatotopic organisations ordered from the thumb up to the little finger, with differences in finger digit specificity between the areas.

Population Receptive Field Modelling

Although these studies were able to produce evidence of somatotopies in S1, they used conventional methods which were limited to only finding the most effective stimulus location on the skin for each voxel. However, as already discussed, neurons in S1 can respond to multiple locations on the skin summed up by their receptive field. Because a voxel reflects the pooled response of a group of neurons, such a receptive field is called a neuronal population receptive field (pRF) in fMRI studies. Methods to estimate a voxel's neuronal pRF could therefore greatly contribute to mapping the somatosensory cortex. A computational approach was first successfully introduced in a visual field mapping study by Dumoulin and Wandell (2008) using pRF models. A similar approach might prove successful in the tactile domain as well.

pRF modelling is a sensory science computational tool used to estimate the response of a population of neurons to certain sensory stimuli. It is similar to a classical GLM approach in that it makes predictions of neural responses to estimate observed data (see appendix). However, instead of predicting an fMRI timeseries for a single stimulus, it generates predictions reflecting responses to all presented stimuli.

A valuable property of pRF modelling is that the key parameters have interpretable units that can be specified in the stimulus frame, namely pRF position and size. A Gaussian function is used to construct a pRF model which takes in a certain dimension of the stimulus as input to generate the predicted BOLD amplitudes. The center of such a function reflects the position of the pRF, while the Gaussian standard deviation, or spread, summarizes its size. Taking tactile stimulus location as an example, one could see the center of the Gaussian function as the area of the skin that provokes the largest BOLD amplitude and the Gaussian spread illustrates the range of surrounding locations to which that particular voxel shows lesser activation. These Gaussian functions are subsequently used to construct predicted fMRI timeseries, which are used in the analysis.

Earlier research has already produced interesting pRF models predicting fMRI timeseries on responses to visual stimuli in the visual cortex and temporal-occipital (TO) boundary (Dumoulin and Wandell 2008; Amano, Wandell, and Dumoulin 2009). More recently, the pRF approach was utilized to reveal a detailed somatotopic organization of the human primary motor cortex (M1) and S1 using motor skill tasks (Schellekens, Petridou, and Ramsey 2018). Although the previously mentioned study already investigated pRF models

in S1, the receptive fields were estimated following finger movements (Schellekens, Petridou, and Ramsey 2018) which might differ from pRF estimates caused by solely tactile stimulation. A pRF model could be estimated based on tactile stimulation using vibrotactile stimulators, which is what we present here.

Aims of the Current Research

The current study investigates whether the pRF approach could be used in fMRI research to further our understanding of the processing of tactile information in the somatosensory cortex. We did so by creating a pRF model that predicts the response of small neuronal populations in S1 to vibrotactile stimuli. Therefore, a method was specifically developed to generate these stimuli using an MRI compatible vibrotactile stimulator (VTS).

In order to determine whether our pRF approach was successful we examined whether our model was able to find a clear somatotopic organisation of the fingers in S1. Based on earlier research we expect to find a clear somatotopy in BA 3b and 1, with the fingers being represented inferior to superior from thumb to little finger. Although BA 2 has lesser specificity to the finger digits, somatotopies have been found in this area and we, thus, expect to find one in this area as well. Furthermore, we investigated whether our model could detect differences in pRF size between the different structures in S1 and between different finger digits. Again, due to finger digit specificity differences we anticipate that receptive fields will be larger in BA 2 compared to BA 3b and 1. Additionally, because mechanoreceptors differ in the types of information that they relay we explored whether the frequency of the stimulus had an effect on cortical responses. Earlier research has suggested that different frequencies are processed by different neural processes (Han et al. 2013).

For the present study we took advantage of the higher signal-to-noise ratio provided by a 7T MRI scanner (see appendix) to obtain high spatial resolution fMRI data, which was used to fit the model.

Methods

Subjects

Five healthy subjects (3 females; ages 23-31 years) were recruited to participate in the research. All volunteers gave written informed consent prior to entering the study. The local ethics committee of University Medical center Utrecht approved the protocol, in accordance with the declaration of Helsinki (2013). The subjects took part in three runs of the experiment where each run of vibrotactile stimulations differed in frequency.

The Vibrotactile Stimulator

To generate the vibrotactile stimuli we used an MR-compatible piezoelectric vibrotactile stimulator (VTS) device created by Dancer Design (http://www.dancerdesign.co.uk/). The VTS setup consisted of an amplifier, one large connecting cable, a stimulator head box, a NI-9264 digital-to-analog converter (DAC) output module (National Instruments), 20 smaller wires and 20 stimulators. The amplifier was used to send electrical currents to the stimulator headbox, which would relay the signal to each of the connected stimulators and generate the vibrotactile stimuli. Because the amplifier is not MR-compatible it could not be in the same room as the MRI scanner. The main stimulator box was therefore connected to it with the large cable through a waveguide in the wall using a radiofrequency (RF) filter. The stimulators were small non-ferrous (thus not magnetic) metal plates in the shape of a triangle encased in plastic and were connected to the stimulator box with smaller wires. The tip of each stimulator served as the point of contact with the skin and covered an area of 1 mm^2 (see figure 3A). In the current study, only 5 stimulators were used. The amplifier was also connected to the DAC device, which was connected to an Acer Aspire 7 A715-71G-76Z5 (Intel Core i7-7700HQ) laptop via a USB cable.

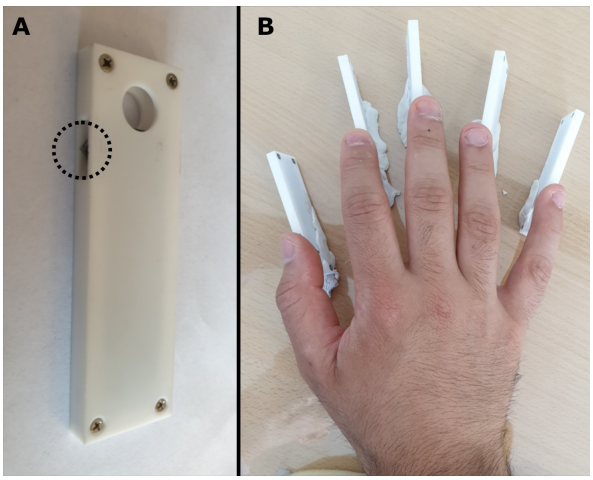

Figure 3: VTS: Left (A) shows a picture of a single encased stimulator, with the tip of the small non-ferrous metallic plate encircled. Right (B) shows a hand on top of the five stimulators, located on the tip of each finger.

The signals were generated by using the Data Acquisition Toolbox in the MatLab programming environment. First, the device and all the output stimulators that were going to be used needed to be registered. Next, a stimulation matrix was created in which each column represented the out-

put of a single stimulator over the course of a full experimental run. Finally, the stimulation matrix was sent as input to the VTS and the stimulators would generate the vibrotactile stimuli accordingly. However, there was a variable delay of a few hundred milliseconds between starting the operation and actual stimulation probably due to buffering. Unfortunately, no solution could be found to this problem.

The Matlab program executing the task waited for a trigger from the scanner before starting the experiment. The slight delay between sending the command and actual exectuion was logged and later used in the analysis.

Task

During the task, vibrotactile stimuli were presented to the five fingertips of the right hand for each subject. The stimulators were attached to a piece of plexiglass using gum strips so that they would be located at the fingertips if a hand would be positioned on top of it (see figure 3B). A piece of foam was placed at the bottom of the plexiglass to enable the subjects to rest their wrist on it comfortably. Before putting the participant in the scanner, the stimulators were adjusted to fit the size of the hand. Finally, medical tape was used for securing the fingers to the stimulators, so it was as easy as possible for subjects not to move their hands and fingers.

Each session consisted of an event-related fMRI design and was repeated for three runs. The difference between these runs was the frequency of the vibrotactile stimuli. It is common to classify vibrotactile stimuli into two types depending on their frequency, namely flutter for stimulation up to 50 Hz and vibration for higher frequency (Han et al. 2013). The first run was at a flutter of 30 Hz, the second run at a vibration of 110 Hz and finally the third at 190 Hz. Each stimulation resulted in a 1mm displacement of the tip of the stimulator on the skin. A run comprised of 8 times 5 stimulations of each fingertip and started with a rest period of 14.4 seconds. The stimulations were 4 s in total, comprising of 0.4 s bursts separated by 0.1 s gaps, so as to limit neuronal adaptation to the vibrotactile stimulus (Yang and O'connor 2014). Time between stimulations was 10 seconds, to allow the BOLD signal to return to baseline. After each 5th stimulation a rest period of 10.4 second occurred (which was chosen due to it being a multiple of the TR of 1.6 s, see scan protocol), although for one subject this was 14.4 seconds. The finger order of stimulations was pseudo-randomized over the whole run in order to create a stimulus design that differed maximally between digits. This minimized the effect of order of stimulation by, for instance, preventing two fingers digits always being stimulated sequentially or one finger digit repeatedly being stimulated 5 times in a row.

During the sessions, participants were asked to count how many times a predetermined finger was stimulated during a certain run to keep their attention. After the run they would be asked for their answer via the intercom. Although the answer would be the same for each experiment (i.e. 8 stimulations), we did not expect participants to stop paying attention due to this predictability within the three runs. Mainly because the subjects might expect the number of stimulations to differ between runs or between fingers.

Scan Protocol

Data were acquired on a 7 T Philips Achieva scanner (Philips Healthcare, Best, Netherlands) with a 32-channel receive headcoil (Nova Medical, MA, USA). The fMRI data was obtained using single shot gradient echo (GE), echo-planar imaging (EPI) with the following parameters: SENSE factor = 3.0, TR = 1600 ms, TE = 27 ms, flip angle = 70 degrees, axial orientation, interleaved slice acquisition, FOV (AP, LR, FH) = $208.8 \times 208.8 \times 41.6$ mm^3. The acquired matrix had the following dimensions: $144 \times 144 \times 26$ with voxel size: $1.45 \times 1.45 \times 1.6$ mm^3. The functional images were acquired from the superior 42 mm of the brain and covered the majority of the frontal and parietal lobes. During the functional image acquisition, 362 scans were made for the first 4 subjects and 372 scans for the last subject. A T1-weighted image of the whole brain ($0.78 \times 0.8 \times 0.78$ mm^3, FOV = $249.6 \times 190.4 \times 249.6$) and a whole-brain proton density image ($0.8 \times 0.8 \times 0.8$ mm^3, FOV = $200 \times 251 \times 190$) were subsequently acquired. Lastly, a functional reversed phase image was acquired (Posterior-Anterior).

Image Processing

The T1-weighted image was divided by the proton-density weighted image to correct for macroscopic field inhomogeneities (Van de Moortele et al. 2009). The corrected T1-weighted image was used to construct grey/white matter surfaces using Freesurfer (https://surfer.nmr.mgh.harvard.edu/ (Dale, Fischl, and Sereno 1999)). These reconstructed brain surfaces are triangulated surface meshes, each triangle consisting of 3 nodes (also called vertices). The entire surface mesh contains more than 100,000 nodes per hemisphere. The functional images were pre-processed using AFNI (https://afni.nimh.nih.gov/). The preprocessing steps included slice time correction, motion correction and EPI phase distortion correction using the

reversed functional image (Buonocore and Gao 1997). Next, the functional images were spatially aligned with the anatomical scans using SPM 12 (https://www.fil.ion.ucl.ac.uk/spm/software/spm12/). All voxels of the preprocessed images that fell in range of the estimated grey matter thickness were subsequently mapped onto the Freesurfer surfaces. Each surface node of the reconstructed surfaces thus obtained its own fMRI timeseries. To eliminate slow signal drift, these timeseries were filtered using a high-pass filter with a cut-off at 5.2×10^{-3}Hz and normalized to represent percentage signal change. Next, all timeseries were denoised using a denoising technique based on the GLM (Kay et al. 2013). Finally, we calculated the average response per finger for each surface node to reduce noise, which resulted in a response spanning 9 TRs per finger. By concatenating these responses from thumb to little finger (1 to 5), we ended up with a reconstructed fMRI timeseries of 45 scans per node.

For our analysis we drew two regions of interest (ROI) for each participant based on earlier research (Rosa Maria Sanchez-Panchuelo et al. 2010; Rosa M Sanchez-Panchuelo et al. 2012) and using the Desikan-Killiany atlas in Freesurfer (Desikan et al. 2006). These ROIs were drawn on the location of the cortical hand area of the contralateral S1. ROI 1 was estimated to contain BA 3b and 1 more anterior on the postcentral gyrus, while ROI 2 covered BA 2 more posterior. These two ROIs were chosen because most studies showed evidence for a somatotopy in ROI 3b and 1, while this was less so for ROI 2 (Iwamura, Tanaka, and Hikosaka 1980; Van Westen et al. 2004). We therefore wanted to investigate somatotopic organizations in these regions separately.

Gaussian pRF Analysis

In fMRI analyses, it is common practice to use a general linear model (GLM) to predict the acquired timeseries of voxels, or in the case of surface-based analysis nodes/vertices (Friston et al. 1995). Such a GLM consists of a stimulus matrix convolved with an HRF, resulting in a design matrix which describes the blood flow after neural activity for each stimulus (see appendix). The strength of each individual column in the design matrix is usually given by β (beta). Although a model of the pRF is a subclass of the GLM, the main difference with the classical approach is that it uses its parameters, position and size, to predict a pattern of BOLD responses to all the stimulations. By considering a large set of pRF parameters for the model, a vast number of predicted timeseries can be generated reflecting BOLD responses to the different stimuli, which are characterized by their amplitude. For each voxel a pRF is then determined by comparing the observed data with the predictions and choosing the parameters that result in the best fit.

The procedure that will be used in the current study to obtain the best pRF fits was first presented by Dumoulin Wandell (2008), in which they describe a measured fMRI timeseries $y(t)$ as:

$$y(t) = \beta \cdot p(t) + \epsilon \tag{1}$$

where $p(t)$ is the predicted BOLD signal, β is a scaling factor that accounts for unknown units, and ϵ is measurement noise. The prediction $p(t)$ is calculated by means of a Gaussian function which takes a certain input and is defined by two parameters, a Gaussian center and Gaussian spread. A neuronal model could be estimated by finding the values for these parameters that best predict the observed timeseries. The input to the Gaussian function is the index of the fingertip that was stimulated, which ranges from 1 to 5 corresponding to the 5 fingertips. Here, we assume a linear relationship between the finger number and the distance between fingertip representations in the brain. This is based on earlier pRF models that discovered a somatotopy in S1 under the same assumption (Schellekens, Petridou, and Ramsey 2018). We can subsequently define the relative amplitude of the Gaussian function corresponding to a specific fingertip stimulation as:

$$g(x) = exp\left(- \frac{(x_0 - x_i)^2}{2 \cdot \sigma^2} \right) \tag{2}$$

where x_i represents the index of the stimulated fingertip (ranging from thumb = 1 to little finger = 5), x_0 the Gaussian pRF center and σ the Gaussian spread. These parameters are all stimulus referred; they relate to the location of the stimulus. The pRF center x_0 corresponds to the preferred fingertip for a given neuronal population and takes a value between 0.5 and 5.5 in steps of 0.25. Thus, x_0 could lie between two fingers, meaning a neuronal population could respond equally to both. Moreover, the possible centers extended by 0.5 in the direction of the thumb and little finger and could thus be located outside the hand. This was allowed to guarantee that the finger digits had equal ranges (i.e. thumb = [0.5:1.5]; index finger = [1.5:2.5]; middle finger = [2.5:3.5]; ring finger = [3.5:4.5]; little finger = [4.5:5.5]). The pRF σ represents the receptive field size of a population of neurons and defines the activity for tactile stimulation of fingertips relative to x_0. It can take a value of 0.25 to 5, also in steps of 0.25. The larger σ gets, the more fingertips it will respond to (figure 4, pRF Model).

Next, we defined the effective task design by multiplying the Gaussian function $g(x)$ with a stimulus matrix $s(x,t)$. The rows of this stimulus matrix represented the five fingertips, while the columns depicted the time in scans (see figure 4, Tactile Task). The value of a column t for a finger x was 1 if the stimulus was apparent at that time and 0 otherwise. Our stimulus matrix reflected a design as if each fingertip was stimulated once from thumb to little finger, due to the reconstructed fMRI timeseries representing average responses per finger digit for each surface node. The stimulus representations were separated by 9 TRs, which resulted in a stimulus matrix with the same length as the fMRI timeseries. After multiplying the new stimulus matrix with $g(x)$, we ended up with a Gaussian model timeseries for each fingertip. By summing over the fingertips, we ended up with pRF response $r(t)$ at each node (figure 4, pRF response), given by:

$$r(t) = \sum_x s(x,t) \cdot g(x) \tag{3}$$

After this, $r(t)$ was convolved with a model of the HRF $h(t)$ to give us the Gaussian model predicted fMRI timeseries $p(t)$ (figure 4, Prediction):

$$p(t) = r(t) * h(t) \tag{4}$$

There were 21 possible Gaussian centers and 20 possible Gaussian spreads. For each combination of center and spread we repeated the steps described above, thus we ended up with a total of $21 \times 20 = 420$ different models.

In the next step, the models were compared to the actual fMRI timeseries. We calculated the Pearson's correlation value ρ for all Gaussian models and the new fMRI timeseries of each surface node. The model with the highest value was considered the best (figure 4, Output) fit. Earlier pRF models subsequently used gradient descent algorithms for all nodes/voxels whose models explained at least 15% of the observed data to find the model parameters that fit even better (Dumoulin and Wandell 2008; Schellekens, Petridou, and Ramsey 2018). However, in the current study we did not think it would contribute significantly to the outcome, due to the initial parameter values already being densely distributed. Thus, we chose a different threshold and only considered nodes that had a $\rho \geq 0.5$ for our statistical analysis, which is the same as 25% variance explained.

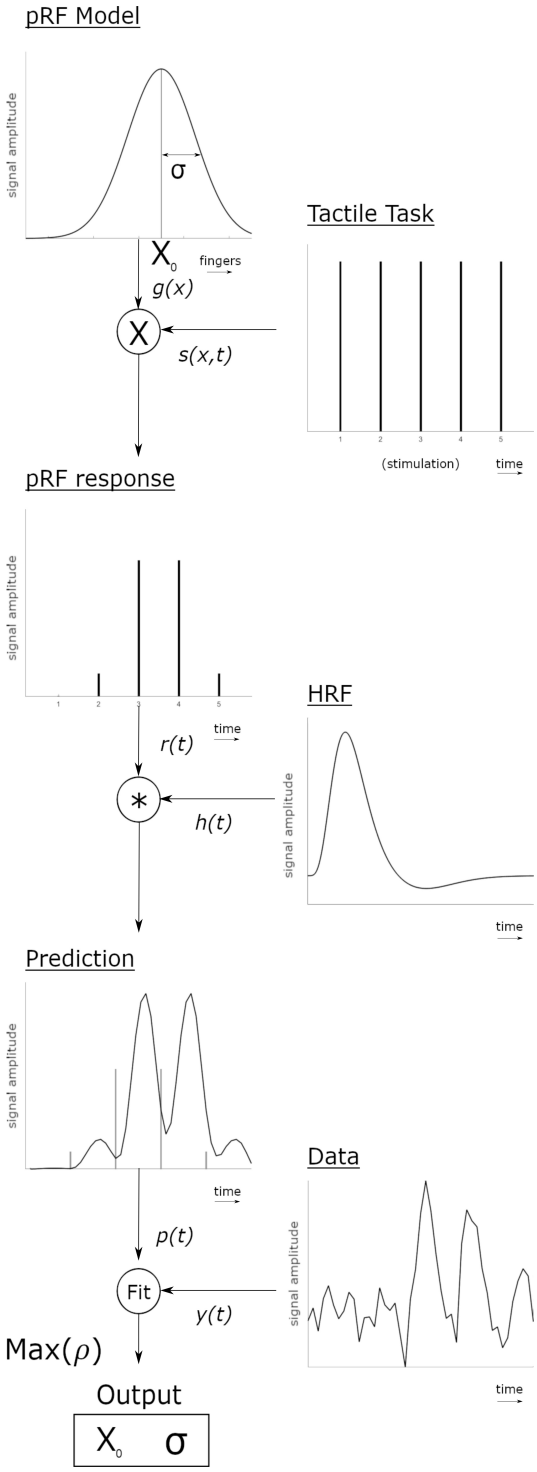

Figure 4: Flowchart Gaussian pRF analysis. For full details see text section Gaussian pRF analysis.

Statistical Analysis

The main goal of this research was to investigate whether a somatotopic organization of the fingertips could be found on the central sulcus and postcentral gyrus in response to vibrotactile stimuli using the pRF approach. Here, a somatotopy is defined as a sequential gradient of Gaussian centers along the cortical surface. The existence of such a sequential gradient was tested by investigating whether there was a linear relationship between

the estimated Gaussian centers and coordinates of the surface nodes that were included. Because the the somatotopies found in earlier studies were most apparent from inferior to superior (Kaas et al. 1979; Van Westen et al. 2004; Besle et al. 2014), we expected a gradient in somatotopic organization to exist along the Y-axes for both ROIs in all 3 runs. We therefore carried out a linear regression where we predicted the Y-coordinates of the surface nodes on the basis of the Gaussian pRF centers for all subjects in each condition. The resulting regression coefficient values would illustrate the linear relation between Gaussian centers and Y-coordinates. A positive regression value would indicate a linear relation with the thumb located inferiorly and the little finger superiorly, while a negative regression demonstrated the exact opposite. Regression values around 0 would be interpreted as no evidence for a linear relation between Gaussian center and the Y-coordinates and would therefore not support the existence of a somatotopy. Whether a linear relationship was significant was based on the probability of finding its R^2 value, which was corrected for multiple comparisons using Bonferroni correction. Additionally, we used a student's t-test over the regression coefficients for both ROIs in all three conditions to look at between-subject effects. Because of our small sample size, we could not use the results of these tests alone to determine the existence of a somatotopy. Therefore, we would combine its outcome with the within-subjects results to reach our conclusion.

We also wanted to examine whether pRF size differences existed between the ROIs and the finger digits. We therefore averaged the Gaussian spread per finger digit per ROI in each condition. We then conducted a repeated measures ANOVA with the factors finger digit (5), frequency (3) and ROI (2) to see whether a single factor or a combination of factors had an effect on pRF size. Furthermore, we wanted to know whether an effect of frequency on neural response could be found, which was characterized by the BOLD amplitude. The amplitude was calculated by regressing the fMRI time series with the predicted model for each surface node and taking the β coefficient. We averaged the BOLD amplitudes similarly to the pRF sizes to calculate a mean amplitude per frequency per finger digit in both ROIs. A repeated measures ANOVA with the frequencies (3), finger digits (5) and ROIs (2) as separate factors investigated whether BOLD amplitudes differed between frequency conditions. Finally, we used another repeated measures ANOVA with the same factors to check whether any of these variables or their combinations had an effect on the number of included surface nodes, which were again averaged per finger per ROI for each condition.

Results

The current study developed a Gaussian pRF model that predicted the fMRI timeseries for tactile stimulation on the fingertips in the primary somatosensory cortex. These timeseries displayed a peak amplitude for the preferred finger of a neuronal population, while amplitudes for stimulating the surrounding digits decreased following a Gaussian spread. Participants reported that they could clearly perceive the vibrotactile stimulations. The acquired fMRI data reflected these subjective perceptions, displaying percentage BOLD signal changes following the stimulations. Subjects had an average of 462 surface nodes (sd = 266) where the model fitted well (i.e. $\rho > 0.5$) located on the cortical hand area along the central sulcus and postcentral gyrus. The percentage BOLD signal changes followed the stimulations of the fingers. Examples for a fitted timeseries can be seen in figure 5 . The collective locations of the preferred finger digit were used to determine whether a somatotopy was present in two ROIs in the contralateral somatosensory cortex. ROI 1 contained BA 3b and 1, while ROI 2 contained BA 2

There was an experimental error during scanning the first subject on the 30 Hz condition. The resulting data was therefore left out of the final analysis.

The results from the pRF analysis demonstrated that a somatotopic organization exists in ROI 1 in each subject (see figure 7A). The representations of preferred finger digits gradually shifted from thumb to little finger on the cortical surface from inferior to superior locations respectively. To support the evidence of a somatotopy a linear regression per stimulus condition was performed for each subject where the predictor variable was the pRF center and the outcome variable was the Y-coordinate on the cortical surface. The outcome for each participant can be found in table 1 below. A significant positive linear relationship was found in ROI 1 for all subjects all conditions. In ROI 2 three individuals displayed a positive linear relationship in the 30 Hz and 110 Hz condition, while one subject displayed a negative relationship in both conditions (see figure 8). One subject did not have data on the 30 Hz condition, as mentioned earlier, and showed no linear relationship in the 110 Hz condition. In the 190 Hz condition four subjects displayed a positive linear relationship, while no relationship was found for the remaining subject.

A student's t-test was also conducted over the

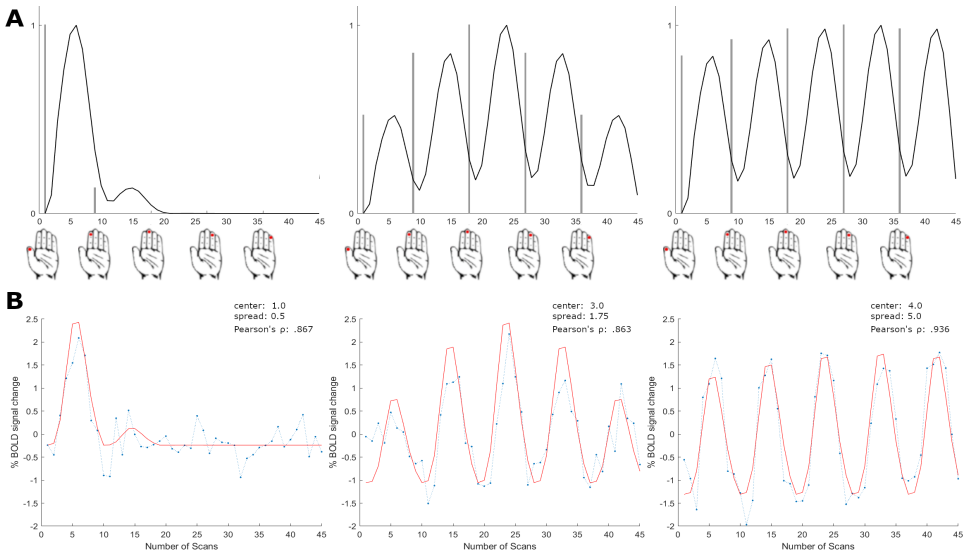

Figure 5: fMRI timeseries with fitted pRF models. The top row (A) displays pRF models with different centers and increasing spread from left to right. Subjects were stimulated for 4 seconds, with a 10 second rest in between. The models were generated to fit the average response per finger. They therefore reflected a design in which each finger was stimulated once from thumb to little finger, which is illustrated by the red dots on the hand. The bottom row (B) illustrates the pRF models (solid red line) fitted to the fMRI timeseries depicting the average responses per finger (blue dotted line+circles). Each response was measured for 9 scans, resulting in a total number of 45 scans

regression coefficients in each condition for group analysis. Based on this test a positive linear relationship was found in ROI 1 for the 30 Hz ($t(3) = 4.955$, $p = .016$) as well as the 110 Hz ($t(4) = 4.323$, $p=0.012$) and 190 Hz ($t(4) =$,$p = 0.015$) condition across subjects. In ROI 2 we found no evidence of a linear relationship in the 30 Hz ($t(3) = 1.417$, $p= .229$), 110 Hz ($t(4) = 1.011$, $p = .369$) and finally the 190 Hz condition ($t(4) = 3.091$, $p = 0.036$), which was not significant due to the Bonferroni correction. These between-subjects results support the idea that a somatotopic organization exists in BA 3b and 1, but not in BA 2. However, due to the small sample size these results cannot be considered as significant evidence.

We also examined the influence of ROI and finger digit on the size of the pRFd (figure 7B). We found that the pRF size (i.e. Gaussian spread) depended on the ROI ($F(1,4) = 41.921$, $p = .004$), resulting in smaller receptive fields for the fingertip representations in ROI 1. For our analysis of pRF size in the finger digits we could not assume sphericity using Mauchly's sphericity test ($p < .001$). We thus observed that finger digits did not differ significantly in their pRF size ($F(4, 16) = 3.094$ $p = 0.104$). A boxplot showing receptive field sizes per finger for both regions can be seen in figure 6.

Next, we tested the effect of frequency on neural responses to the vibrotactile stimuli. No differences in BOLD amplitude were found between the different frequency conditions ($F(2, 8)= 0.663$ $p=.557$). Thus, the BOLD amplitude in response to the different frequencies remained similar.

Finally, we did not find evidence for an effect of frequency ($F(2, 6) = .841$, $p = .427$), ROI ($F(1, 3) = .801$, $p = .437$) or digit ($F(4, 12) = .954$, $p =.467$) on the number of included surfaces nodes for the analysis. However, in some participants the number of included nodes did differ between frequencies (see figure 7), but this was variable between subjects.

Discussion

The main goal of the current study was to investigate whether a pRF approach could be used in fMRI research to study the topographic organization of the somatosensory cortex. Specifically, we measured neural responses to vibrotactile stimulation of the fingertips in the cortical hand location of the contralateral primary somatosensory cortex (S1). We subdivided this area into ROI 1, which was assumed to consist of BA 3b and 1, and ROI 2, which we estimated to contain BA 2.

The sample size (5) of the current study was too small to conclude a significant result on the between-subjects tests. However, by combining the results of these statistical tests with the individual outcomes of the linear regressions, we conclude that we found evidence for a positive linear relationship between pRF center and Y-coordinate on the cortical surface in ROI 1 for all frequency conditions. We thus demonstrate that a somatotopy exists in BAs 3b and 1, where the representations of the fingers moved gradually from the thumb most inferior up to the little finger more superior. Fol-

Frequency	P	ROI 1	ROI 1	ROI 1	ROI 2	ROI 2	ROI 2
		Beta	R^2	p-value	Beta	R^2	p-value
30 Hz	1	-	-	-	-	-	-
	2	0.93	.188	<.0001	-1.05	.072	<.0001
	3	2.20	.229	<.0001	1.22	.087	<.0001
	4	2.87	.696	<.0001	3.44	.595	<.0001
	5	1.96	.633	<.0001	1.04	.169	<.0001
110 Hz	1	2.35	.683	<.0001	-0.80	.001	.354
	2	0.62	.101	<.0001	-0.74	.027	.011
	3	1.45	.361	<.0001	0.96	.126	<.0001
	4	3.31	.712	<.0001	1.74	.222	<.0001
	5	1.89	.619	<.0001	1.61	.448	<.0001
190 Hz	1	2.51	.553	<.0001	1.17	.203	.001
	2	0.51	.059	.005	0.14	.002	.51
	3	1.25	.177	<.0001	0.96	.062	<.0001
	4	3.23	.751	<.0001	2.85	.54	<.0001
	5	2.10	.387	<.0001	1.94	.49	<.0001

Table 1: : Table containing the linear regression Beta-coefficient, R^2 and p-value for each participant (P) per frequency condition in both ROIs.

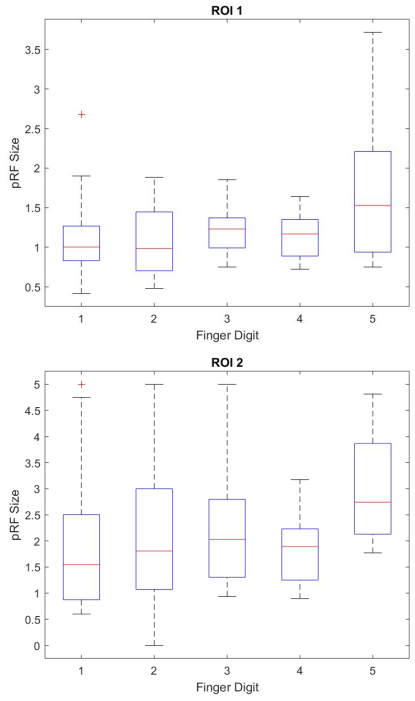

Figure 6: Two boxplots displaying the Gaussian spreads per finger for the different ROIs. ROI 1 was argued to contain BA 3b and 1 which had an average spread of 1.25 over all fingers. ROI 2 depicted BA 2, which displayed an average spread of 2.3. The red line indicated the median pRF spread for each finger, while the blue box illustrated the area between the 25th and 75th percentile. The whiskers extended to the most extreme values. Variance between the finger digits differed too much to assume sphericity.

lowing the same line, we could not conclude the same for BA 2 due to outcome of the t-tests and the different linear relationships we observed in ROI 2.

We also showed that pRF sizes in BA 2 were significantly larger than those in BA 3b and 1, suggesting greater overlap of finger digit representations in this area. We found no differences in pRF sizes between the individual finger digits. Furthermore, our current data does not support the notion that the frequency of the stimulus affects neural responses in S1, which meant that the BOLD amplitudes in response to vibrotactile stimuli of different frequencies were similar. Finally, no evidence was found that the number of included surface nodes differed between digit, frequency or the different areas.

Evidence for the existence of somatotopies was based on the preferred finger digits of the neuronal populations, characterized by the centers of their pRF. In our current model we fitted the pRF centers on a range of predetermined parameter values (0.5 – 5.5), which meant that such a center could be located between two fingers. Although this might seem counterintuitive, there is a logical explanation. We measured the responses of a population of neurons, which can contain more than 100,000 neurons (Lent et al. 2012)). There is therefore a high probability that such a population contains neurons that have different preferred finger digits, resulting in multiple finger representations in the population. Moreover, surface nodes could have their pRF center outside of the fingers (i.e. <1 or >5). As mentioned earlier, these values were allowed to guarantee equal range between fingers. These surface nodes could still contain neurons with a receptive field on either the thumb or little finger and were therefore still considered when defining somatotopic organization.

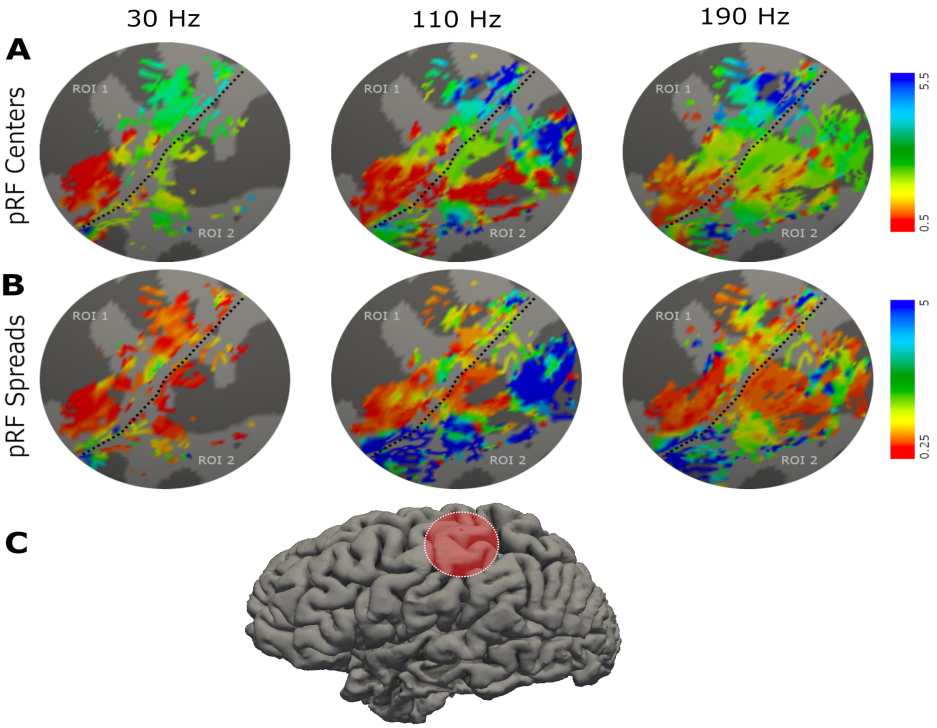

Figure 7: The somatotopic maps found for one subject in all three stimulus conditions. Three maps (A) display the pRF centers, with a gradual color scaling from red (thumb) to blue (little finger) representing the pRF centers for each frequency. Similar maps were produced to display the spreads (B). Here the color scaling represented the amount of spread. The dotted line in the middle represented the border between ROI 1 and ROI 2. The location of the maps were in agreement with the cortical hand representation of S1 on the postcentral gyrus (C).

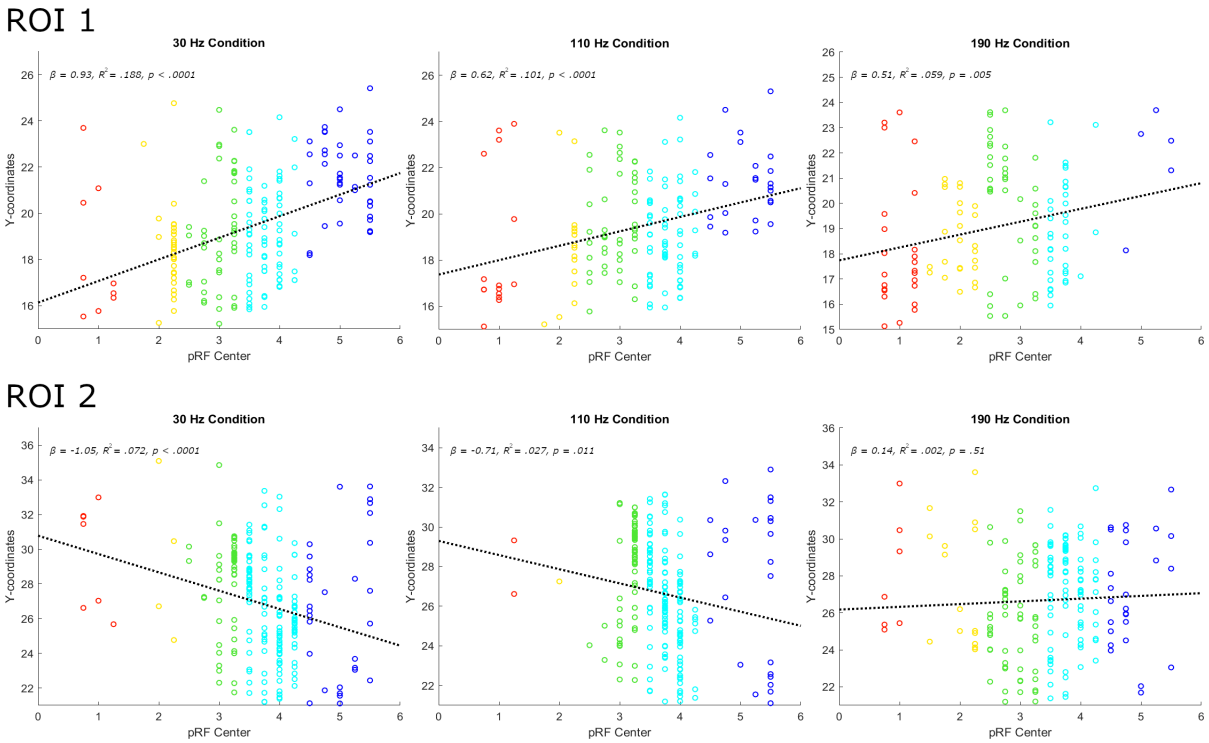

Figure 8: Linear regression plots for the two ROIs displaying the linear relationship between pRF center and Y-coordinate on the surface of the cortex in subject 2. pRF centers are color coded based on the finger digit they represent (i.e. thumb = red, index finger = yellow, middle finger = green, ring finger = cyan and little finger = blue). These particular figures show the results of subject 2, which shows positive linear relationships in ROI 1. The data for ROI 2 displayed either a negative relationship or no relationship at all.

The somatotopies discovered in BA 3b and 1 are in line with the findings of earlier research on macaques (Iwamura, Tanaka, and Hikosaka 1980) and fMRI studies on humans (Van Westen et al. 2004; Nelson AJ 2008; Rosa Maria Sanchez-Panchuelo et al. 2010). These studies were only able to distinguish a clear somatotopic organization in BA 3b and 1, which had the same inferior to superior distribution of fingers we present here. These studies were unable to find a similar somatotopy in BA 2, which might indicate that a somatotopic organization along the inferior-superior axis does not exist in this area . However, microelectrode studies on macaques have already established that each cytoarchitectonic structure in S1 has its own independent representation of body parts (Kaas et al. 1979). Furthermore, the more recent study by Martuzzi and colleagues (2014) actually was able to establish a somatotopy of the fingers in BA 2 based on fMRI data. Our current data did not provide enough support for the existence of a somatotopy in BA 2 on a group level. However, looking at the data on a single-subject level shows that three participants did display a clear somatotopy similar to the one found in BA 3b and 1 in all three frequency conditions (i.e. a positive linear relationship between pRF center and Y-coordinate on the cortical surface, see Table 1). Moreover, the data that contradicted the existence of a somatotopy in BA 2 came mostly from a subject X (see figure 8). Some complication during the experiments in this particular subject might have affected the resulting data, which in turn influenced the data on a group level and the subsequent conclusion. Thus, even though the present study could not provide substantial evidence in support of a somatotopy of the finger digits in BA 2, we cannot exclude it exists either. Combining the three BAs, we did not find that a specific digit was represented more than others within the topographic maps. This was based on the number of included surface nodes for the analysis. This contrasts with earlier findings in which the thumb was represented to a greater extent than the other fingers(Besle et al. 2014). However, some topographic maps may have lost possible finger representations due to the initial thresholding at $\rho \geq 0.5$, which resulted in incomplete maps (see figuer 9. The number of included surface nodes differed between subjects and those that had more complete topographic maps did seem to show a larger representation of the thumb (see figure 7, the red centers).

As mentioned in the introduction, we did not only want to investigate the preferred finger digit for a neuronal population but also to what other digits it responds. In the earlier mentioned macaque study, researchers found that neurons in BA 3b and 1 responded mostly to a specific finger digit while neurons in BA 2 could respond to up to five (Iwamura, Tanaka, and Hikosaka 1980)). They could therefore not find evidence of a somatotopic organization in the latter. Other non-human primate studies found that specificity even differed between BA 3b and 1, which led them to conclude that specificity gradually decreases BA 3b to BA 2 (Sur, Merzenich, and Kaas 1980). The fMRI study in which researchers did find a somatotopy had a similar conclusion (Martuzzi et al. 2014). They based the specificity per area on the average BOLD response to tactile stimulation of each finger digit within the five finger digit representations in BAs 3b, 1 and 2. Finger digit representations in BA 3b only displayed a significant BOLD response to their specific finger digit, while this specificity decreased slightly in BA 1 and was at its lowest in BA 2, in which representations could overlap 5 fingers. In the current study the specificity for each surface node was described by its pRF, with large pRFs signifying low specificity. Our results are, thus, in agreement with the findings that finger digit specificity in BA 2 is lower than in BA 3b and 1. However, because BA 3b and 1 were in the same ROI we did not test for differences in pRF size between these areas. We can, therefore, not confirm the existence of a gradual specificity decrease between areas. Nevertheless, the larger pRFs in BA 2 could still be viewed as support for this gradual decrease. These larger pRFs might imply that the neuronal populations in BA 2 include neurons that respond to stimulations of multiple finger digits, similar to the findings in the monkey study (Iwamura, Tanaka, and Hikosaka 1980). However, it could also mean that neurons tuned to a single digit start to mix together within these populations. For example, a surface node could mostly contain neurons that respond to only the thumb, but also some neurons that only respond to the index finger. Either way, it does indicate that this area probably plays a role in integrating information from the different digits (Hyvarinen J 1978). Tactile information from the different fingers is needed to interact with objects and manipulate them. Tactile information might enter the somatosensory cortex in BA 3b, after which it is delivered to BA 2 where this information is combined and subsequently sent to other areas for more complex processing (Hoechstetter et al. 2001). Indeed, non-human primate studies did find that the BA 3b receives most of its input directly from the thalamus, after which it is projected to BA 1 and 2 (Felleman and Essen 1991). Although we did find differences in pRF size between the cortical areas, we could not demonstrate the same between finger digits. Earlier research did not report any findings

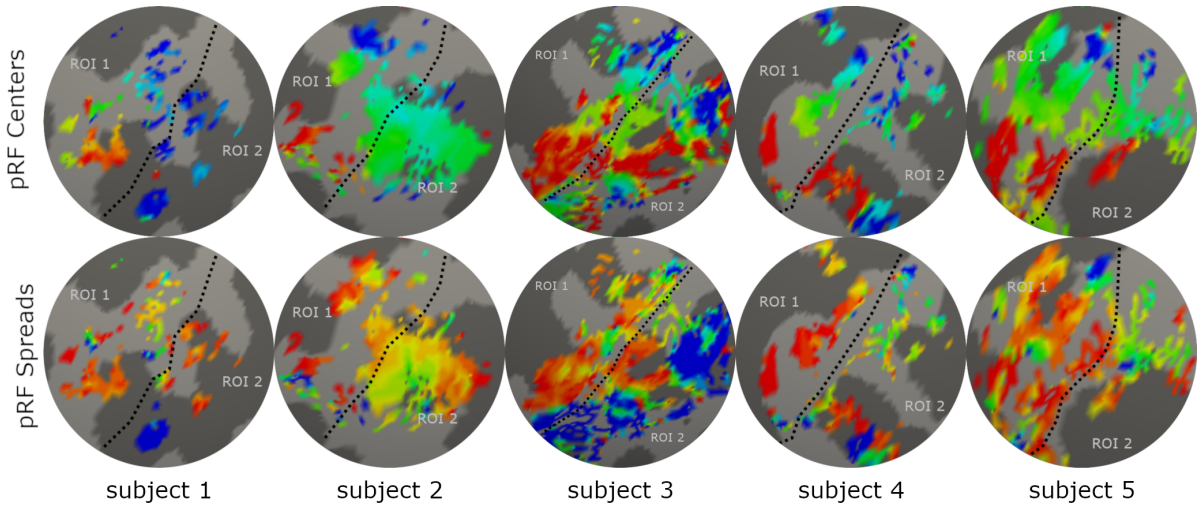

Figure 9: Maps showing the topographic organization for all subjects in the 110 Hz frequency condition. It is clear to see that some subjects demonstrated more finger representations than others.

on the subject, thus we conclude that we cannot provide evidence that pRF size differs between digits.

Our results concerning pRF sizes emphasizes the advantage of using pRF models for researching S1. Instead of carrying out separate analyses to determine the finger digit specificity of different brain areas based on mean BOLD responses, the models we present here were able to estimate this specificity for each individual surface node.

Apart from focusing on the location of a vibrotactile stimulus on the skin, we also examined a possible frequency dependency of neural responses. The idea that frequency could have an effect on neural response was based on the fact that different mechanoreceptors are involved in relaying vibrotactile information to the CNS depending on the frequency, namely Meissner corpuscles for flutter and Pacinian corpuscles for vibration. This dimension of the stimulus was not captured in the model but was compared between experimental runs.

Our findings contradict outcomes of earlier research. Animal studies showed that mean firing rate of neurons in S1 remained constant in response to flutter, while it declined during vibration (Whitsel et al. 2001). Studies in humans also showed more activation to flutter than to vibration in S1 (Harrington and Downs 2001; Chung et al. 2013)).

A possible reason could be that the relatively small stimulus area on the skin (1 mm) was not able to activate a large enough neural population to detect a frequency dependency. In other words, when stimulating a small area on the skin the measured BOLD signal might simply depict a neural response to any vibrotactile stimulus. Activation in S1 might only become frequency dependent if a large enough area on the skin is stimulated. Indeed, the aforementioned study by Chung and colleagues (2013) used a stimulus with a size of 10×10 mm^2. Using multiple stimulators per finger digit might produce a different outcome. They also stimulated the fingers for 30s, which might imply that the effects of frequency might build over extended periods of time. Also, the data for the different frequencies was acquired through independent scans. Possible variation between the scans might have influenced the results. Still, even on the small area of the skin and during the 4s stimulations, the different frequencies of the vibrotactile stimuli could clearly be distinguished. Thus, another explanation for our data might be that frequency is mostly processed in other areas of the brain, for instance in the secondary somatosensory cortex (S2) (Ryun et al. 2017). This could mean that input from Meissner and Pacinian corpuscles are processed equally in S1.

Study Limitations

There were a few limitations in the current study which might have influenced the outcome. One of these limitations was the delay we observed between instructing the MatLab program to start the experiment and the actual start, which could be up to one second. We attempted to account for this problem by including the delay times in the analysis, which were estimated using the program's internal stopwatch function and subsequently logged. These estimations were no guarantees that we knew the actual time delay. This uncertainty might have caused the timing of our predictions to be slightly incorrect, which would influence the resulting data. Actual responses to the vibrotactile stimulation might have been missed by wrongly timing the stimulations in the stimu-

lus matrix. However, the current result shows that the timing would not have been off by too much. Still, a more precise method would be desirable.

Furthermore, in the present study we had a limited number of subjects, which meant that a single subject could greatly influence the resulted outcome, which probably happened in the current study. Moreover, the fMRI data for one of the subjects in the 30 Hz condition was considered unusable, reducing the sample size even more. Without a sufficiently large participant group we could not establish a somatotopy based on a t-test over regression coefficients and had to combine it with individual measurements to establish our conclusions. Increasing the sample size is therefore advised. Finally, as mentioned earlier, some finger representations within the somatotopy might have been lost in a few subjects. Although it is possible that these representations are simply not present, it is more likely that the model was unable to detect them because the average signal in response to stimulation was not strong enough due to noise. Increasing the number of stimulations per finger digit might be able to resolve this. Also, lowering the initial threshold could detect more finger representations which currently might have been left out of the analysis.

Future Work

Possible future studies should firstly address the limitations we encountered described in the last paragraph. Thus, a study containing more subjects in which each fingertip is stimulated more than eight times might be able to find more significant support for somatotopies in BAs 3b, 1 and 2. Furthermore, we investigated differences in pRF size between BA 2 and BAs 3 and 1. However, as discussed, possible differences in pRF size between BA 3b and 1 might also exist. Dividing S1 in three ROIs and using the same pRF model might be able to find supporting evidence for this difference.

In the current study we focused our attention on the fingertips, which resulted in an interdigit somatotopy. One of the advantages of pRF models is that they can be multidimensional, which means our model could be extended by including the area of the individual fingers along the phalanges. Such a study could result in a full somatotopic map of the cortical hand area in S1 combined with corresponding pRF sizes. This would greatly contribute to our general knowledge on how tactile processing achieved.

Of course, our pRF method can also be applied to map other parts of the body and to investigate somatotopic organization in different parts of the brain involved in tactile processing, such as S2 (Ruben et al. 2001; Longo, Azañón, and Haggard 2010).

Furthermore, other characteristics of the vibrotactile stimulus could also be examined with a pRF model, such as the frequency. Presently, we studied its effect by comparing results between different experiments. A pRF model that predicts responses to stimuli of different frequencies could help to identify brain regions specialized in processing that particular feature. A multidimensional model combining both location of the stimulus and frequency could also be contrived.

Finally, at the beginning of this paper we discussed how research into tactile processing in humans could contribute to new technologies. More specifically, we discussed how implementing the sense of touch in robots could contribute to the goal of developing fully autonomous systems. Some research into the subject has aimed their attention on generating artificial somatotopic representations in robots (Cannata, Denei, and Mastrogiovanni 2010). This type of research might benefit from the findings we presented in this study concerning receptive field differences between areas. For instance, by generating somatotopies where a specific area is only concerned with the input from tactile sensors, after which it is relayed to adjacent areas for further processing.

Conclusion

In the current study we have shown that the pRF approach can be extended to map the somatosensory cortex. We did so by developing a model that predicted the responses to vibrotactile stimuli in S1. Our data demonstrated a somatotopy in BA 3b and 1 similar to those found in earlier studies. Although we were unable to significantly establish the same in BA 2, individual results did indicate that such a somatotopic organization exists in this area. Further investigation is required. Next to the somatotopies, we found that pRF size differed between cytoarchitectonic architectures in line with findings from previous research. This aspect of our model highlighted the advantage of using the pRF approach by describing specificity to a finger digit for each neuronal population. Combining the found somatotopic organization with the pRF sizes gives a more detailed map of the brain. These maps can help create artificial somatotopies or assist those that have suffered damage in touch perception. For instance, knowing that neuronal populations in BA 3b and 1 are very specific to a single finger digit could mean that focussing recovery on these areas might help people regain perception in the fingertips.

Now that we have shown that pRF models can be used to map S1, introducing it to other areas involved in touch is the next step. This will result in an even better understanding of tactile perception. Moreover, different dimensions of tactile stimuli can be investigated, like vibrational frequency. Combining different dimensions in a single model is also possible and might shed light on possible interactions of these dimensions.

Thus, the current study was the first step in investigating touch in the somatosensory cortex using pRF models, the extension of which might be able to improve our knowledge of tactile processing even more.

Acknowledgements

I would like to express my deepest gratitude to dr. Natalia Petridou and dr. Wouter Schellekens for supervising me during this project. Through their guidance I have learned a lot and I could not have succeeded without their continuous support. Furthermore, I want to thank dr. Ben Harvey for his feedback and patience during the writing of this final paper.

References

Abraira, Victoria E and David D Ginty (2013). "The sensory neurons of touch". In: *Neuron* 79.4, pp. 618–639.

Amano, Kaoru, Brian A Wandell, and Serge O Dumoulin (2009). "Visual field maps, population receptive field sizes, and visual field coverage in the human MT+ complex". In: *Journal of neurophysiology* 102.5, pp. 2704–2718.

Antfolk, Christian et al. (2013). "Sensory feedback in upper limb prosthetics". In: *Expert review of medical devices* 10.1, pp. 45–54.

Besle, Julien et al. (2014). "Event-related fMRI at 7T reveals overlapping cortical representations for adjacent fingertips in S1 of individual subjects". In: *Human brain mapping* 35.5, pp. 2027–2043.

Buonocore, Michael H and Lisheng Gao (1997). "Ghost artifact reduction for echo planar imaging using image phase correction". In: *Magnetic resonance in medicine* 38.1, pp. 89–100.

Cannata, Giorgio, Simone Denei, and Fulvio Mastrogiovanni (2010). "Tactile sensing: Steps to artificial somatosensory maps". In: *19th International Symposium in Robot and Human Interactive Communication*, pp. 576–581.

Chung, Yoon Gi et al. (2013). "Frequency-dependent patterns of somatosensory cortical responses to vibrotactile stimulation in humans: A fMRI study". In: *Brain research* 1504, pp. 47–57.

Clark, Sharon A et al. (1988). "Receptive fields in the body-surface map in adult cortex defined by temporally correlated inputs". In: *Nature* 332.6163, p. 444.

Dahiya, Ravinder S et al. (2010). "Tactile Sensing-From Humans to Humanoids." In: *IEEE Trans. Robotics* 26.1, pp. 1–20.

Dale, Anders M, Bruce Fischl, and Martin I Sereno (1999). "Cortical surface-based analysis: I. Segmentation and surface reconstruction". In: *Neuroimage* 9.2, pp. 179–194.

Desikan, Rahul S et al. (2006). "An automated labeling system for subdividing the human cerebral cortex on MRI scans into gyral based regions of interest". In: *Neuroimage* 31.3, pp. 968–980.

Dumoulin, Serge O and Brian A Wandell (2008). "Population receptive field estimates in human visual cortex". In: *Neuroimage* 39.2, pp. 647–660.

Ekstrom, Arne (2010). "How and when the fMRI BOLD signal relates to underlying neural activity: the danger in dissociation". In: *Brain research reviews* 62.2, pp. 233–244.

Felleman, Daniel J. and David C. Van Essen (1991). "Distributed Hierarchical Processing in the Primate Cerebral Cortex". In: *Cerebral Cortex* 1.1, pp. 1–47.

Friston, Karl J et al. (1995). "Characterizing evoked hemodynamics with fMRI". In: *Neuroimage* 2.2, pp. 157–165.

Geyer, Stefan, Axel Schleicher, and Karl Zilles (1997). "The somatosensory cortex of human: cytoarchitecture and regional distributions of receptor-binding sites". In: *Neuroimage* 6.1, pp. 27–45.

Greenspan, Joel D and Robert H LaMotte (1993). "Cutaneous mechanoreceptors of the hand: experimental studies and their implications for clinical testing of tactile sensation". In: *Journal of Hand Therapy* 6.2, pp. 75–82.

Han, Sang Woo et al. (2013). "Evaluation of somatosensory cortical differences between flutter and vibration tactile stimuli". In: *2013 35th Annual International Conference of the IEEE Engineering in Medicine and Biology Society (EMBC)*. Vol. 2013, pp. 4402–4405.

Harrington, Gregory S. and J. Hunter Downs (2001). "FMRI mapping of the somatosensory cortex with vibratory stimuli: Is there a dependency on stimulus frequency?" In: *Brain Research* 897.1, pp. 188–192.

Herweg, Andreas et al. (2016). "Wheelchair control by elderly participants in a virtual envi-

ronment with a brain-computer interface (BCI) and tactile stimulation". In: *Biological psychology* 121, pp. 117–124.

Hoechstetter, Karsten et al. (2001). ""Interaction of Tactile Input in the Human Primary and Secondary Somatosensory Cortex—A Magnetoencephalographic Study"". In: *NeuroImage* 14.3, pp. 759–767.

Hyvarinen J, Poranen A (1978). "Movement-sensitive and direction and orientation-selective cutaneous receptive fields in the hand area of the post-central gyrus in monkeys." In: *The Journal of Physiology* 283.1, pp. 523–537.

Iadecola, Costantino (2004). "Neurovascular regulation in the normal brain and in Alzheimer's disease". In: *Nature Reviews Neuroscience* 5.5, p. 347.

Iggo, A and KH Andres (1982). "Morphology of cutaneous receptors". In: *Annual review of neuroscience* 5.1, pp. 1–31.

Iwamura, Yoshiaki, Michio Tanaka, and Okihide Hikosaka (1980). "Overlapping representation of fingers in the somatosensory cortex (area 2) of the conscious monkey". In: *Brain research* 197.2, pp. 516–520.

Johansson, Roland S and Åke B Vallbo (1983). "Tactile sensory coding in the glabrous skin of the human hand". In: *Trends in neurosciences* 6, pp. 27–32.

Johnson, Kenneth O (2001). "The roles and functions of cutaneous mechanoreceptors". In: *Current opinion in neurobiology* 11.4, pp. 455–461.

Kaas, Jon H (2004). "Somatosensory system". In: *The human nervous system*, pp. 1059–1092.

Kaas, Jon H et al. (1979). "Multiple representations of the body within the primary somatosensory cortex of primates". In: *Science* 204.4392, pp. 521–523.

Kandel, Eric R et al. (2000). *Principles of neural science*. Vol. 4. McGraw-hill New York.

Kay, Kendrick et al. (2013). "GLMdenoise: a fast, automated technique for denoising task-based fMRI data". In: *Frontiers in neuroscience* 7, p. 247.

Klatzky, Roberta L, Susan J Lederman, and Victoria A Metzger (1985). "Identifying objects by touch: An "expert system"". In: *Perception & psychophysics* 37.4, pp. 299–302.

Lent, Roberto et al. (2012). "How many neurons do you have? Some dogmas of quantitative neuroscience under revision". In: *European Journal of Neuroscience* 35.1, pp. 1–9.

Logothetis, Nikos K (2008). "What we can do and what we cannot do with fMRI". In: *Nature* 453.7197, p. 869.

Longo, Matthew R., Elena Azañón, and Patrick Haggard (2010). "More than Skin Deep: Body Representation beyond Primary Somatosensory Cortex." In: *Neuropsychologia* 48.3, pp. 655–668.

Lumpkin, Ellen A and Michael J Caterina (2007). "Mechanisms of sensory transduction in the skin". In: *Nature* 445.7130, p. 858.

Martuzzi, Roberto et al. (2014). "Human finger somatotopy in areas 3b, 1, and 2: a 7T fMRI study using a natural stimulus". In: *Human brain mapping* 35.1, pp. 213–226.

McGlone, Francis and David Reilly (2010). "The cutaneous sensory system". In: *Neuroscience & Biobehavioral Reviews* 34.2, pp. 148–159.

Nelson AJ, Chen R (2008). "Digit somatotopy within cortical areas of the postcentral gyrus in humans". In: *Cerebral Cortex* 18.10, pp. 2341–2351.

Ogawa, Seiji et al. (1990). "Brain magnetic resonance imaging with contrast dependent on blood oxygenation". In: *proceedings of the National Academy of Sciences* 87.24, pp. 9868–9872.

Pacchierotti, Claudio, Domenico Prattichizzo, and Katherine J Kuchenbecker (2015). "Cutaneous feedback of fingertip deformation and vibration for palpation in robotic surgery". In: *IEEE Transactions on Biomedical Engineering* 63.2, pp. 278–287.

Pamungkas, DS and K Ward (2016). "Electro-tactile feedback system to enhance virtual reality experience". In:

Penfield, Wilder and Edwin Boldrey (1937). "Somatic motor and sensory representation in the cerebral cortex of man as studied by electrical stimulation". In: *Brain* 60.4, pp. 389–443.

Robles-De-La-Torre, Gabriel (2006). "The importance of the sense of touch in virtual and real environments". In: *Ieee Multimedia* 13.3, pp. 24–30.

Rothwell, JC et al. (1982). "Manual motor performance in a deafferented man". In: *Brain* 105.3, pp. 515–542.

Ruben, J. et al. (2001). "Somatotopic Organization of Human Secondary Somatosensory Cortex". In: *Cerebral Cortex* 11.5, pp. 463–473.

Ryun, Seokyun et al. (2017). "Tactile Frequency-Specific High-Gamma Activities in Human Primary and Secondary Somatosensory Cortices". In: *Scientific Reports* 7.1, p. 15442.

Sanchez-Panchuelo, Rosa Maria et al. (2010). "Mapping human somatosensory cortex in individual subjects with 7T functional MRI". In: *Journal of neurophysiology* 103.5, pp. 2544–2556.

Sanchez-Panchuelo, Rosa M et al. (2012). "Within-digit functional parcellation of Brodmann areas of the human primary somatosensory cortex using functional magnetic resonance imag-

ing at 7 tesla". In: *Journal of Neuroscience* 32.45, pp. 15815–15822.
Schellekens, Wouter, Natalia Petridou, and Nick F Ramsey (2018). "Detailed somatotopy in primary motor and somatosensory cortex revealed by Gaussian population receptive fields". In: *Neuroimage* 179, pp. 337–347.
Sur, Mriganka, Michael M Merzenich, and Jon H Kaas (1980). "Magnification, receptive-field area, and" hypercolumn" size in areas 3b and 1 of somatosensory cortex in owl monkeys." In: *Journal of neurophysiology* 44.2, pp. 295–311.
Tamè, Luigi et al. (2012). "The contribution of primary and secondary somatosensory cortices to the representation of body parts and body sides: an fMRI adaptation study". In: *Journal of Cognitive Neuroscience* 24.12, pp. 2306–2320.
Van de Moortele, Pierre-François et al. (2009). "T1 weighted brain images at 7 Tesla unbiased for Proton Density, T2 contrast and RF coil receive B1 sensitivity with simultaneous vessel visualization". In: *Neuroimage* 46.2, pp. 432–446.
Van Westen, Danielle et al. (2004). "Fingersomatotopy in area 3b: an fMRI-study". In: *BMC neuroscience* 5.1, p. 28.
Whitsel, B. L. et al. (2001). "Frequency-dependent response of SI RA-class neurons to vibrotactile stimulation of the receptive field". In: *Somatosensory and Motor Research* 18.4, pp. 263–285.
Yang, Hongdian and Daniel H O'connor (2014). "Cortical adaptation and tactile perception". In: *Nature neuroscience* 17.11, p. 1434.

Appendix Principles of fMRI

The present study used functional magnetic resonance imaging (fMRI) to estimate neural activity in the human brain. MRI is an imagining technique that quantifies the magnetic properties of matter placed in an MRI scanner to create a three-dimensional image. When a body is placed in the scanner, a strong external magnetic field is applied which causes the magnetic fields of the nuclei within the body to align with it (Berger 2002). Subsequent manipulations of the external field using radiofrequency (RF) pulses causes a signal to be emitted, which can be measured at each single data point of the image, called a voxel (i.e. a volume element or 3D pixel). The signal strength at each voxel depends on the magnetic properties (e.g. magnetic susceptibility) of the underlying body tissue. The contrast of the image is determined by the signal strength, with high contrast indicating a strong signal and vice-versa. By comparing measurements of different voxels an anatomical image can be created. However, changes over time at individual voxels can also be obtained, which is the basis for functional MRI.

One method of using fMRI to measure brain activity is by taking advantage of the difference in magnetic susceptibility between oxygenated and deoxygenated blood. Oxygenated blood is less susceptible to the external magnetic field created by the scanner than deoxygenated blood, resulting in a stronger signal. This signal is otherwise known as the blood-oxygen-level-dependent (BOLD) signal and can be used to map the cerebral blood flow (CBF)(Seiji Ogawa et al. 1990). When neurons activate, they require glucose and oxygen as source for energy. Because neurons do not have their own storage for these energy substrates, they are delivered to the activated area through a dense web of blood vessels following a process called neurovascular coupling(Iadecola 2004). However, less oxygen is consumed than is supplied, which results in an excess of oxygenated blood in the active area and therefore an increase in BOLD signal (S. Ogawa et al. 1992). This increase is not concurrent with the neural activity, but occurs some time later following a predictable time course characterised by the hemodynamic response function (HRF, see figure 2 in the paper) (Logothetis and Wandell 2004). Therefore, BOLD signal often correlates strongly with underlying neural activity (Ekstrom 2010). Changes in neural activity can be estimated by measuring the signal over time, which results in observed activation patterns in the brain.

The specificity of the BOLD signal is determined by the architecture of the microvasculature in the brain. Blood is provided to the neurons through the capillaries, which are very small blood vessels. Therefore, the signal should reflect oxygenation changes in these capillary beds rather than the surrounding larger vessels to reflect underlying neural activity. In other words, large vessels within a voxel can cause noise and might result in mis localisation of activation patterns. One solution is to increase the external magnetic field strength generated by the scanner, which is expressed in units of Tesla (T). This decreases the signal coming from large vessels and thus contributes to a higher signal-to-noise ratio and increases the spatial resolution and specificity (Seiji Ogawa et al. 1990). For this reason, a 7T high field MRI scanner was used in the current study.

In short, fMRI is an imaging technique that measures neural activity on the basis of the BOLD signal. This signal increases when oxygenated blood flows into the activated area following metabolic activity and is summarized in the HRF. The next step is understanding how fMRI studies are performed and how the subsequent data is analysed.

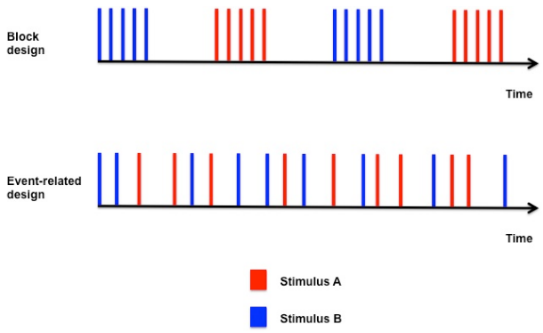

Figure 1: Different designs with two stimuli (red and blue). Borrowed from Schmucker-von Koch 2013.

fMRI Designs and Analysis

When conducting fMRI research, the goal is to measure brain responses to certain stimuli. There are several experimental designs used in fMRI research, the most common being univariate block design and event-related design (see Figure 1). In experiments following the block design, different stimuli are represented for an extended amount of time following each other, sometimes interspersed by a short pause. In even-related design experiments, the stimuli are presented shortly and with a lot of time in between. The way these stimuli are presented is often described in a binary stimulus matrix, in which the columns represent different stimuli and the rows account for the time. Thus, a row would have a value of 1 if it was present at a certain time and 0 otherwise. The obtained data is commonly analysed using computational mod-

els, due to the predictable relationship between the BOLD signal and neural activity. Most often a classic general linear model (GLM) is used to predict the acquired timeseries of voxels (Friston et al. 1995). First, each column of the stimulus matrix is convolved with the HRF to create predicted timeseries. Convolution is a mathematical operation whereby one function modifies the shape of another function by calculating the integral of the product of the two functions. This results in a design matrix where each column depicts a predicted fMRI timeseries to a single stimulus. These stimulus timeseries are then used as factors in a liner regression predicting the actual data per voxel. The strength of each factor is the given a value β (beta). These β-values are then used to determine a certain T-value illustrating which stimulus is preferred for each individual voxel.

References

Berger, Abi (2002). "How does it work?: Magnetic resonance imaging". In: *BMJ* 324.7328, pp. 35–35.

Ekstrom, Arne (2010). "How and when the fMRI BOLD signal relates to underlying neural activity: the danger in dissociation". In: *Brain research reviews* 62.2, pp. 233–244.

Friston, Karl J et al. (1995). "Characterizing evoked hemodynamics with fMRI". In: *Neuroimage* 2.2, pp. 157–165.

Iadecola, Costantino (2004). "Neurovascular regulation in the normal brain and in Alzheimer's disease". In: *Nature Reviews Neuroscience* 5.5, p. 347.

Logothetis, Nikos K. and Brian A. Wandell (2004). "Interpreting the BOLD Signal". In: *Annual Review of Physiology* 66.1, pp. 735–769.

Ogawa, Seiji et al. (1990). "Brain magnetic resonance imaging with contrast dependent on blood oxygenation". In: *proceedings of the National Academy of Sciences* 87.24, pp. 9868–9872.

Ogawa, S. et al. (1992). "Intrinsic signal changes accompanying sensory stimulation: functional brain mapping with magnetic resonance imaging". In: *Proceedings of the National Academy of Sciences of the United States of America* 89.13, pp. 5951–5955.

Schmucker-von Koch, Joseph (2013). "Functional Magnetic Resonance Imaging Understanding the technique and addressing its ethical concerns with a future perspective http://ec.europa.eu/research/participants/data/ref/h2020/other/hi/ethics-guide-fmri$_e n.pdf$". In: *http://ec.europa.eu/research/participants/data/ref/h2020/other/hi/ethics-guide-fmri$_e n.pdf$*.